BIOLOGY OF REPRODUCTION **80,** 804–812 (2009)
Published online before print 7 January 2009.
DOI 10.1095/biolreprod.108.072603

# Dynamic Nuclear Organization of Constitutive Heterochromatin During Fetal Male Germ Cell Development in Mice[1]

**Hirotaka Yoshioka,[2,4] John R. McCarrey,[5] and Yukiko Yamazaki[3,4]**

*Institute for Biogenesis Research,[4] John A. Burns School of Medicine, University of Hawaii, Honolulu, Hawaii*
*Department of Biology,[5] University of Texas at San Antonio, San Antonio, Texas*

## ABSTRACT

**In mice, male germ cells enter mitotic arrest beginning at 13.5 days postcoitum (dpc), and remain suspended in the $G_0/G_1$ cell cycle stage until after birth. During this period, male germ cells undergo extensive epigenetic reprogramming, which is essential for their subsequent function as male gametes. A global reorganization and spatial clustering of constitutive heterochromatin has been implicated in epigenetic plasticity during cellular differentiation. Here, we have studied the dynamics of heterochromatin in fetal (12.5–19.5 dpc) and neonatal (4 days postpartum) male germ cells. We monitored constitutive heterochromatin-specific markers, and observed changes in the association of histone H3 trimethylation of lysine 9 (H3K9me3), binding of heterochromatin protein 1, and patterns of 4′,6-diamino-2-phenylindole staining in pericentric regions of chromosomes, along with a coincident loss of chromocenters in fetal prospermatogonia during mitotic arrest. We also observed a transient loss of H3K9me3 associated with major and minor satellite repeat sequences, plus inactivation of histone methyltransferases (*Suv39h1* and *Suv39h2*), and transient activation of histone demethylase (*Jmjd2b*) in these same cells. These epigenetic changes were correlated with relocation of centromeric regions toward the nuclear periphery in prospermatogonia during mitotic arrest. Taken together, these results show that constitutive heterochromatin undergoes dramatic reorganization during prespermatogenesis. We suggest that these dynamic changes in heterochromatin contribute to normal epigenetic reprogramming of the paternal genome in fetal prospermatogonia suspended in the $G_0/G_1$ stage, and that this also represents an epigenomic state that is particularly amenable to reprogramming.**

*constitutive heterochromatin, early development, epigenetic, gamete biology, gametogenesis, histone modifications, mitotic arrest, prespermatogenesis, spermatogenesis*

## INTRODUCTION

In mammals, the precursors of gametogenesis are the primordial germ cells (PGCs), which, in the mouse embryo, arise from the proximal layer of the epiblast at 6.25 days postcoitum (dpc) [1]. By 8.5 dpc, PGCs enter the embryo proper, then proliferate and migrate to the genital ridges by 11.5 dpc [2, 3]. The sex-determining gene on the Y chromosome, *Sry*, is first expressed in the male genital ridges at 10.5 dpc [4] to initiate a cascade of gene expression that leads to testis development [5, 6]. By 12.5 dpc, morphological sex differentiation occurs in the developing male gonads to form testicular cords [5]. Sexual differentiation of the germ cells initiates 1 day later, at 13.5 dpc. Female germ cells begin to enter meiosis, while male germ cells, termed type M prospermatogonia at this stage, become enclosed by the developing testicular cords and continue mitotic cell division. By 15.5 dpc, these male germ cells stop dividing and enter mitotic arrest. They are called type $T_1$ prospermatogonia at this stage, and they remain suspended in the $G_0/G_1$ phase of the cell cycle until 3–4 days postpartum (dpp), when, as type $T_2$ prospermatogonia, they reinitiate a burst of mitotic activity [2, 7].

During the initial stages of germ cell sex differentiation in the fetus, the germline genomes in both sexes undergo dynamic epigenetic reprogramming, including erasure and resetting of sex-specific genomic imprints [8–19]. This epigenetic plasticity is essential to the process of germ cell sex differentiation, and the acquisition of developmental competence by both the sperm and the oocyte genomes [19]. Nuclear transfer (cloning) has been used to assess the correlation of epigenetic plasticity and developmental potential of fetal germ cell genomes [20–24]. We and others found that germ cell nuclei taken from fetuses at 8.5–10.5 dpc were fully competent to support development of viable cloned offspring based on inherited epigenetic programming that had not yet been erased [23, 24], whereas germ cell nuclei recovered at 11.5 dpc or later were developmentally incompetent [20–22]. This loss of developmental competence was correlated with the initial erasure, and subsequent biallelic resetting of genomic imprints in the germline genomes in both sexes, resulting in identical imprinting (or lack thereof) on both alleles of each imprinted gene in these cells. The lack of proper allele-specific imprinting in cloned offspring leads to developmental defects, especially during late fetal development, as evidenced by a relatively high population of blastocysts cloned from germ cells that successfully implanted in the womb, but then suffered from severe developmental retardation or death by midgestation stages [21, 22]. Despite these defects manifest during fetal development, the donor germ cell nuclei were competent to direct preimplantation development of cloned embryos, and even early postimplantation development of cloned fetuses to varying extents.

[1]Supported by National Institutes of Health grant HD042772 to J.R.M. and Y.Y.
[2]Correspondence and current address: Hirotaka Yoshioka, Department of Oral Growth and Developmental Biology, Hiroshima University Graduate School of Biomedical Sciences, Hiroshima 734-8553, Japan. FAX: 81 82 257 5621; e-mail: hirotaka@hiroshima-u.ac.jp
[3]Correspondence: Yukiko Yamazaki, Institute for Biogenesis Research, John A. Burns School of Medicine, University of Hawaii, 651 Ilalo Street, Honolulu, HI 96813. FAX: 808 692 1962; e-mail: yyamazak@hawaii.edu

Received: 6 August 2008.
First decision: 4 September 2008.
Accepted: 23 December 2008.

eISSN: 1259-7268 http://www.biolreprod.org
ISSN: 0006-3363

Interestingly, when 15.5-dpc male germ cell nuclei were used as donors for cloning, 100% of the cloned, two-cell embryos developed to the morula/blastocyst stage, and 26% of these developed to midgestation fetuses following transfer to surrogate dams [22]. By comparison, only 54% of two-cell embryos cloned from 12.5-dpc male germ cell nuclei developed to the morula/blastocyst stage, and only 5.7% of these formed midgestation fetuses following embryo transfer [22]. Lee et al. also reported that the recovery of morula/blastocyst stage embryos, and their subsequent implantation rates were higher in embryos cloned from 14.5- to 15.5-dpc PGCs than in those cloned from 12.5- to 13.5-dpc PGCs [21]. Because $G_0/G_1$ is the most suitable cell cycle stage for the nuclear transfer, type $T_1$ prospermatogonia at 15.5 dpc, which are suspended in a $G_0/G_1$ mitotic arrest, may possess relatively greater developmental competence for directing preimplantation development than mitotically active type M prospermatogonia at 12.5 dpc, even though neither was able to sustain normal development of fetuses during postimplantation stages.

We ascribed the differences in initial developmental competence of embryos cloned from mitotically active (type M) or mitotically inactive (type $T_1$) prospermatogonia to differential capacities of nuclei from each of these cell types to respond to reprogramming cues upon transfer into an enucleated oocyte, but wondered how these differences are manifest in these donor nuclei. A major aspect of epigenetic reprogramming involves changes in chromatin [19, 25]. Therefore, to begin to investigate the different capacities for reprogramming potential displayed by mitotically active and inactive male germ cells, respectively, we undertook a study of the global organization and epigenetic modifications of constitutive heterochromatin in these two cell types.

In mammals, constitutive heterochromatin primarily encompasses the pericentric regions of chromosomes, and is important for chromosome segregation [26]. Pericentric heterochromatin is mainly composed of a repetitive DNA sequence, called the major satellite repeat, which flanks the centromeric domain consisting of minor satellite repeats, and is characterized by hypoacetylated histones and trimethylation at lysine 9 of histone H3 (H3K9me3) [27]. These modified states of histones have been implicated in the maintenance of heterochromatin protein (CBX5, also known as HP1) binding at pericentric heterochromatin, and in transcriptional silencing and centromere function [28–30]. In interphase nuclei, major satellites on different chromosomes are associated in clusters, called chromocenters, whereas the corresponding minor satellites are located in surrounding domains that associate with centromeric proteins [31].

Initially, constitutive heterochromatin was thought to be stable in composition and transcriptionally inert [29]. However, several lines of recent evidence now show that dynamic reorganization occurs in constitutive heterochromatin, and that this contributes to epigenetic plasticity during cellular development and differentiation. In particular, pluripotent embryonic stem (ES) cells show dynamic organization of heterochromatin [32, 33]. In these cells, CBX5 and linker histones, key proteins involved in maintaining a heterochromatic state, exhibit transient binding to target chromatin domains [32]. In certain terminally differentiated cells, such as quiescent B lymphocytes, pericentric heterochromatin domains are reorganized into large clusters following mitotic stimulation [34]. Extensive clustering of heterochromatin also takes place during differentiation of myoblasts into myotubes, a process that is correlated with increased DNA methylation. This process has also been shown to require histone deacetylase activity, and can be induced by overexpression of methyl-CpG binding domain proteins [35, 36]. This illustrates that global reorganization, spatial clustering, and epigenetic modifications of constitutive heterochromatin are associated with major changes in epigenetic plasticity during cellular differentiation.

In the study described here, we investigated correlations between global organization and epigenetic modifications of constitutive heterochromatin, and mitotic activity (at 12.5–13.5 dpc or 4 dpp) or inactivity (at 15.5–19.5 dpc) in developing male germ cells. In addition, we also examined these same parameters in undifferentiated ES cells to determine which may be correlated with genomic pluripotency. Our results show that developing prospermatogonia undergo dramatic changes in the manner in which constitutive heterochromatin is organized and epigenetically modified. We suggest that these changes may correlate with the significant changes in epigenetic plasticity and developmental capacity that we have previously observed in these cell types.

## MATERIALS AND METHODS

### Mice Used and Collection of Tissues

Transgenic mice expressing germ cell-specific green fluorescent protein (GFP) driven by the *Pou5f1* gene promoter/enhancer (Tg OG2) were generated by microinjecting (CBA/CaJ × C57BL/6J) F2 zygotes (a generous gift from Dr. J.R. Mann, University of Melbourne, Melbourne, Australia) [11]. Female CD1 mice were mated with male Tg OG2 mice to produce (CD1 × OG2) F1 hybrid fetuses and pups. Mating was assessed by the presence of a vaginal plug on the following morning, and recorded as Embryonic Day 0.5 (0.5 dpc). Gonads were dissected in Hepes-Dulbecco modified Eagle medium (Invitrogen, Carlsbad, CA) with 20% fetal bovine serum, and incubated in saline/ethylenediaminetetraacetic acid (EDTA) plus glucose solution for 10 min at room temperature to dissociate germ cells, as previously described [37]. After incubation, gonads were gently pipetted and filtered through a 40-μm cell strainer (BD Biosciences, San Jose, CA) to prepare a single-cell suspension. Fetal male germ cells were isolated on the basis of GFP expression using either fluorescence-activated cell sorting (FACS) or individual picking by micromanipulator, as described in each section below. Neonatal male germ cells at 4 dpp were isolated on the basis of morphological characteristics.

Cumulus cells were collected from B6D2F1 (C57BL/6 × DBA/2) mice. Female mice were induced to superovulate by consecutive injections of equine chorionic gonadotropin (5 IU; Calbiochem, San Diego, CA) and human chorionic gonadotropin (5 IU; Calbiochem) 48 h apart. At 14 h after human chorionic gonadotropin injection, oocyte-cumulus complexes were collected from oviducts. Ovulated oocyte-cumulus complexes were treated with 0.1% hyaluronidase (300 U/mg; Sigma-Aldrich, St. Louis, MO) for 5 min to disperse cumulus cells.

Mouse ES cells (R1 line) were maintained as previously described [38]. All relevant experimental protocols were reviewed and approved by the Institutional Animal Care and Use Committee of the University of Hawaii.

### Immunocytochemistry and Interphase Fluorescence In Situ Hybridization

GFP-positive male germ cells, cumulus cells, and ES cells were picked using a fluorescence microscope (Olympus, Center Valley, PA) equipped with a micropipette, and placed on UltraStick slides (Ted Pella, Inc., Redding, CA). For immunocytochemistry, cells were fixed with 2% paraformaldehyde, and were washed three times with PBS containing 0.1% Tween 20 (PBS-Tween). Slides were then incubated in PBT (PBS containing 0.15% bovine serum albumin and 0.1% Tween 20) plus 5% goat serum for 60 min at 37°C prior to overnight incubation with one of the following antibodies: H3K9me3 (Abcam, Cambridge, MA), 1:200; or CBX5 (HP1α; Millipore, Billerica, MA), 1:100. Thereafter, slides were washed three times for 5 min in PBS-Tween, and incubated with secondary antibodies (Alexa Fluor 568 goat anti-rabbit IgG, 1:500, or Alexa Fluor 568 goat anti-mouse IgG, 1:100 [Invitrogen]) for 60 min in PBT at 37°C. After washing in PBS-Tween, slides were mounted in Vectashield with 4′,6-diamino-2-phenylindole (DAPI; Vector Laboratories Inc., Burlingame, CA). Immunofluorescence was visualized using a FluoView 1000 confocal microscope (Olympus). For interphase fluorescence in situ hybridization (FISH), cells were fixed with 3:1 methanol:acetic acid and baked

for 3 h at 65°C. Slides were denatured in 70% formamide/2× saline-sodium citrate (SSC) at 70°C for 3 min, and then dehydrated in a cold 70%/85%/100% ethanol series for 1 min each. The Cy-3-labeled mouse pancentromeric probe (Open Biosystems, Huntsville, AL) was denatured at 75°C for 10 min. The labeled probe was dropped onto the denatured cells, covered with Parafilm (Alcan Packaging, Neenah, WI), and incubated at 37°C overnight in a humidified chamber. After hybridization, the slides were washed in 50% formamide/2× SSC at 37°C, 2× SSC, and 1× SSC for 15 min each, and once briefly in PBS. The slides were mounted in Vectashield with DAPI (Vector Laboratories Inc.). Signals were observed and photographed using a FluoView 1000 confocal microscope (Olympus).

### Chromatin Immunoprecipitation Assay

Chromatin immunoprecipitation (ChIP) assays were performed as previously described [39], with minor modifications. The GFP-positive male germ cells were sorted using a FACSAria cell sorter (BD Biosciences). After sorting, the purity of GFP-positive cells was ≥95%. A total of $3 \times 10^4$ GFP-positive male germ cells was mixed with $1 \times 10^7$ *Drosophila melanogaster* SL2 cells (Invitrogen). Cells were fixed in a final concentration of 1% formaldehyde for 10 min at room temperature, and then the reaction was stopped by addition of 125 mM glycine. Cells were washed twice in NB buffer (15 mM Tris-HCl, pH 7.4, 60 mM KCl, 15 mM NaCl, 5 mM $MgCl_2$, 0.1 mM ethyleneglycol-bis-(β-aminoethyl ether)-N,N′-tetraacetic acid, 1 mM PMSF, 5 mM sodium butyrate, Halt protease inhibitor cocktail [Pierce Biotechnology, Inc., Rockford, IL]). Cells were then resuspended in NB buffer plus 0.2% Igepal CA-630 and left on ice for 15 min. After washing nuclei with NB buffer plus 0.32 M sucrose, the nuclear pellets were resuspended in micrococcal nuclease (MNase) digestion buffer (20 mM Tris-HCl, pH 8.0, 5 mM NaCl, 2.5 mM $CaCl_2$, 2% Triton X-100), and digested with 30 U MNase (TAKARA Bio USA, Madison, WI) for 5 min at room temperature. The MNase reaction was stopped by adding a similar volume of MNase stop buffer (20 mM Tris-HCl, pH 8.0, 20 mM EDTA, 295 mM NaCl, 0.2% SDS), and incubating at 4°C overnight with agitation. After centrifugation to remove cellular debris, the chromatin solution was incubated with anti-H3K9me3 (Abcam) antibody and Dynabeads protein A (Invitrogen) at 4°C overnight with agitation. The beads were washed several times, and the attached immune complexes were eluted with a buffer containing 1% SDS, 10 mM dithiothreitol and 0.1 M $NaHCO_3$. Cross-links were reversed by the addition of 5 M NaCl and incubation at 65°C for 5 h. The samples were then treated with RNase A for 30 min and proteinase K for 1 h, and DNA was purified by phenol-chloroform extraction and ethanol precipitation. DNA was quantified using a NanoDrop spectrophotometer (Thermo Fisher Scientific, Waltham, MA) and analyzed by quantitative PCR.

### Quantitative Real-Time PCR for ChIP Assay

Quantitative PCR analysis was carried out with DNA precipitated by ChIP using the MyiQ single-color real-time PCR detection system (Bio-Rad, Hercules, CA) with iQ SYBR Green Supermix (Bio-Rad). Each PCR assay was performed in duplicate. PCR primers were as follows: for major satellite repeats, 5′-GACGACTTGAAAAATGACGAAATC-3′, 5′-CATATTCCAGGTCCTTCAGTGTGC-3′; for minor satellite repeats, 5′-CATGGAAAATGATAAAAACC-3′, 5′-CATCTAATATGTTCTACAGTGTGG-3′ [34, 40]. Relative amounts of DNA in the input and bound fractions were determined from cycle threshold ($C_T$) values, using a standard curve generated from DNA of known concentrations. Values for enrichment were calculated as the average of two independent ChIP experiments conducted on germ cells at 12.5 and 19.5 dpc, and three or more experiments conducted on germ cells at 13.5, 15.5, and 17.5 dpc. Statistical analyses were performed using the Student *t*-test.

### Quantitative Gene Expression Analysis

Quantitative real-time PCR was performed using the MyiQ single-color real-time PCR detection system (Bio-Rad) with iQ SYBR Green Supermix (Bio-Rad). A total of 200–400 GFP-positive germ cells were collected as one set, and cDNA was synthesized using the Superscript III Cells Direct cDNA synthesis system (Invitrogen). We used three sets of germ cells from each stage for each gene expression assay. PCR primers were as follows (forward and reverse, respectively): for *Suv39h1*, 5′-TGTGATGCCAGGCACTTGGT-3′, 5′-TGGGCTCCACCTTTGTGGTT-3′; for *Suv39h2*, 5′-TTGGAGTGCCAGGCAGAGTG-3′, 5′-CACTGTCATCGGGGCTTGTG-3′; for *Jmjd2b*, 5′-GTGGCTGAGGGCAGGAGAAA-3′, 5′-GTGCAGACTGGGCCTGTGAA-3′, for *Actb*, 5′-CGCCATGGATGACGATATCG-3′, 5′-CGAAGCCGGCTTTGCACATG-3′. The relative expression of target mRNAs was calculated from target $C_T$ values and *Actb* $C_T$ values using the standard curve method. Results were normalized to *Actb* gene expression and calibrated according to the result from 12.5 dpc male germ cells. Data are presented as means of three replicate analyses of each cell type. Statistical analyses were performed using the Student *t*-test.

## RESULTS

### Epigenetic Changes in Constitutive Heterochromatin in Male Germ Cells

Pericentric heterochromatin, the major component of constitutive heterochromatin, can be easily visualized in interphase nuclei by the fluorochrome, DAPI, and by immunostaining of H3K9me3 and CBX5. In mouse somatic cells, pericentric heterochromatin domains cluster together and form higher-order chromatin structures, called chromocenters, which are visualized as DAPI-dense foci [31]. Since constitutive heterochromatin architecture and higher-order structures are important for epigenetic plasticity [32–36], we characterized this phenotype in male germ cells during fetal (12.5–19.5 dpc) and neonatal (4 dpp) periods. Male germ cells were stained with DAPI, and immunostained to detect H3K9me3 and CBX5, to reveal the global organization of constitutive heterochromatin.

Three different staining patterns were observed during male germ cell development (Fig. 1, A and B). In the first pattern, H3K9me3 and CBX5 staining was confined to small, discrete foci, coincident with intense DAPI staining, and were widely distributed in the nuclei (Fig. 1, A and B, 12.5 dpc panels). In the second pattern, staining revealed punctuate foci of heterochromatin, which primarily localized around the nuclear periphery (Fig. 1, A and B, 13.5 dpc panels). In the third pattern, staining showed a loss of chromocenters and a generally diffuse staining of heterochromatin, with some enrichment at the nuclear periphery (Fig. 1, A and B, 15.5 dpc panels). As shown in Figure 2, the distribution of these three staining patterns of H3K9me3 and CBX5 varied as a function of the developmental stage of male germ cells. At 12.5–13.5 dpc, examples of all three staining patterns were observed (Fig. 1, A and B, 12.5–13.5 dpc panels). As development proceeded, the proportion of germ cells with diffuse staining (the third pattern) gradually increased, such that, between 15.5 and 19.5 dpc, all of the cells showed this diffuse localization of H3K9me3 and CBX5 throughout the nuclei, with loss of chromocenter formation, as observed by DAPI staining (Fig. 1, A and B, 15.5–19.5 dpc panels). Interestingly, in postnatal male germ cells at 4 dpp, the pattern reverted to that observed at 12.5–13.5 dpc (Fig. 1, A and B, 4 dpp panels).

These epigenetic changes in nuclear organization of heterochromatin occurred coincidentally with the transition from mitotically active type M prospermatogonia to mitotically arrested type $T_1$ prospermatogonia, and then to mitotically active type $T_2$ prospermatogonia, respectively. During the late fetal period (15.5–19.5 dpc), type $T_1$ prospermatogonia are characterized by mitotic arrest and by a period of significant epigenetic reprogramming [8–19]. To determine if the heterochromatin organization that we observed in these cells is a common feature of all cell types arrested at the $G_0/G_1$ phase of the cell cycle, we examined adult cumulus cells, which are arrested at the $G_0/G_1$ stage at the time of ovulation [41]. Interestingly, as shown in Figure 1C, H3K9me3 and CBX5 in mitotically *inactive* cumulus nuclei were accumulated in DAPI-dense pericentric heterochromatin domains similar to those seen in mitotically *active* male germ cells at 12.5 dpc (Fig. 1, A and B, 12.5 dpc panels). Thus, in two separate experiments, 41 of 41 (100%) and 33 of 36 (96%) cumulus cells showed a punctate

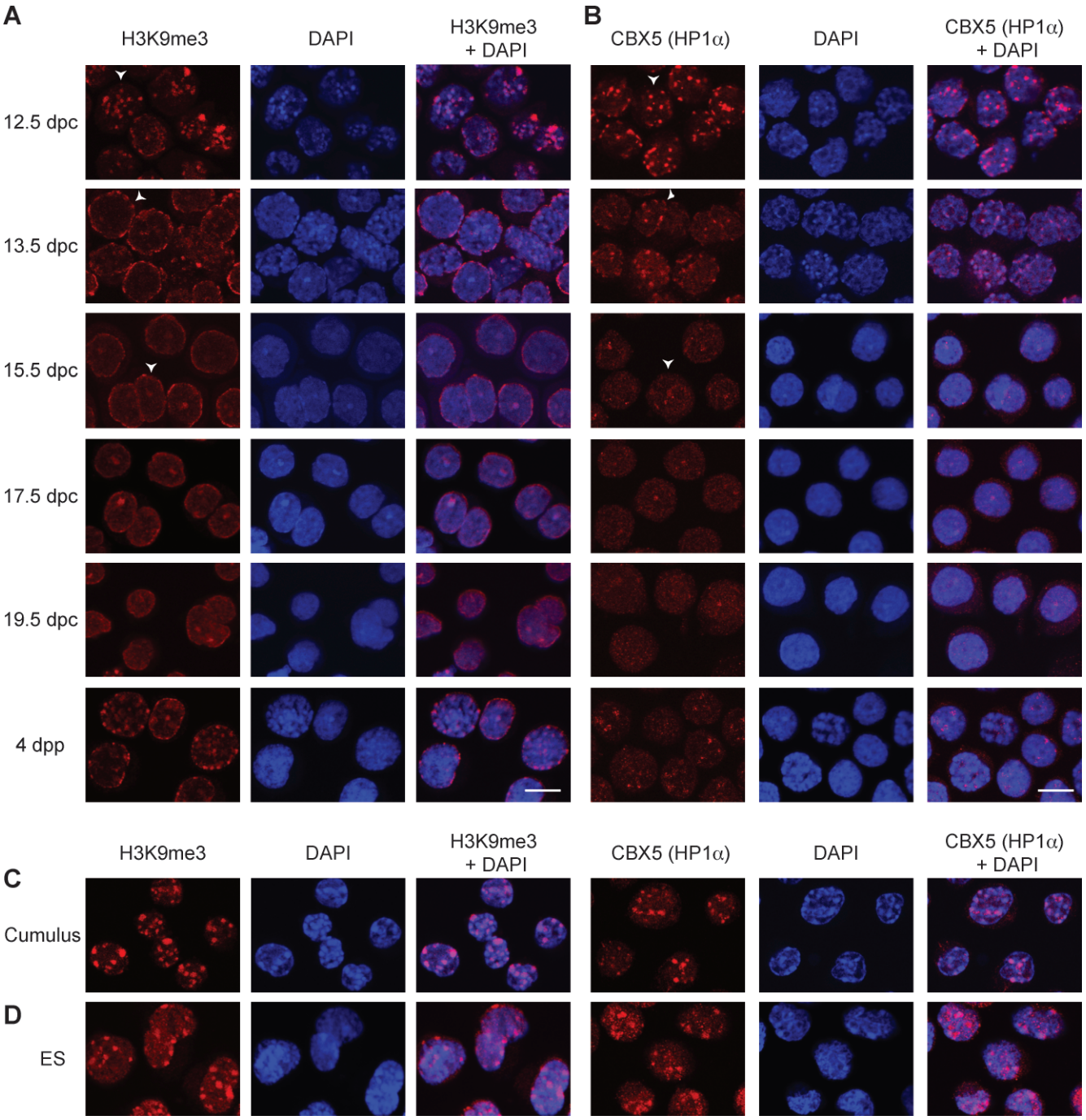


FIG. 1. Dynamic organization of epigenetic heterochromatin states during prespermatogenesis. **A**) The kinetics of H3K9me3 in fetal and neonatal male germ cells. Male germ cells were isolated from fetuses at 12.5, 13.5, 15.5, 17.5, and 19.5 dpc, and neonates at 4 dpp, and stained with anti-H3K9me3 antibody (red) and DAPI (blue). Arrowheads in the panels of 12.5, 13.5, and 15.5 dpc cells indicate the typical staining patterns of the H3K9me3 as punctate, punctate perinuclear distribution, and diffuse, respectively. **B**) The kinetics of CBX5 in fetal and neonatal male germ cells. Male germ cells were stained with anti-CBX5 antibody (red) and DAPI (blue). Arrowheads in the panels of 12.5, 13.5, and 15.5 dpc cells indicate the typical staining patterns for CBX5 as punctate, punctate perinuclear distribution, and diffuse, respectively. **C** and **D**) Immunofluorescence detection of H3K9me3 (left panels) and CBX5 (right panels) in cumulus cells (**C**) and in ES cells (**D**). Bars = 10 μm.

pattern of H3K9me3 and CBX5, respectively (data not shown). To determine if a transition to the heterochromatin organization seen in type $T_1$ prospermatogonia is characteristic of cells that have undergone epigenetic reprogramming to achieve pluripotency, we next examined undifferentiated, pluripotent ES cells. By immunostaining for H3K9me3 and CBX5, 120 of 154 (78%) and 33 of 50 (66%) ES cells, respectively, showed the same pattern of organization of constitutive heterochromatin as that detected in type M prospermatogonia (Fig. 1, A and B, 12.5 dpc panels) and in adult cumulus cells (Fig. 1D). The remaining ES cells showed almost no staining for either H3K9me3 or CBX5, and were therefore distinct from type $T_1$ prospermatogonia (data not shown). Thus, we observed the same pattern of heterochromatin organization in four different cell types (mitotically active type M prospermatogonia at 12.5 dpc; mitotically active type $T_2$ prospermatogonia; mitotically

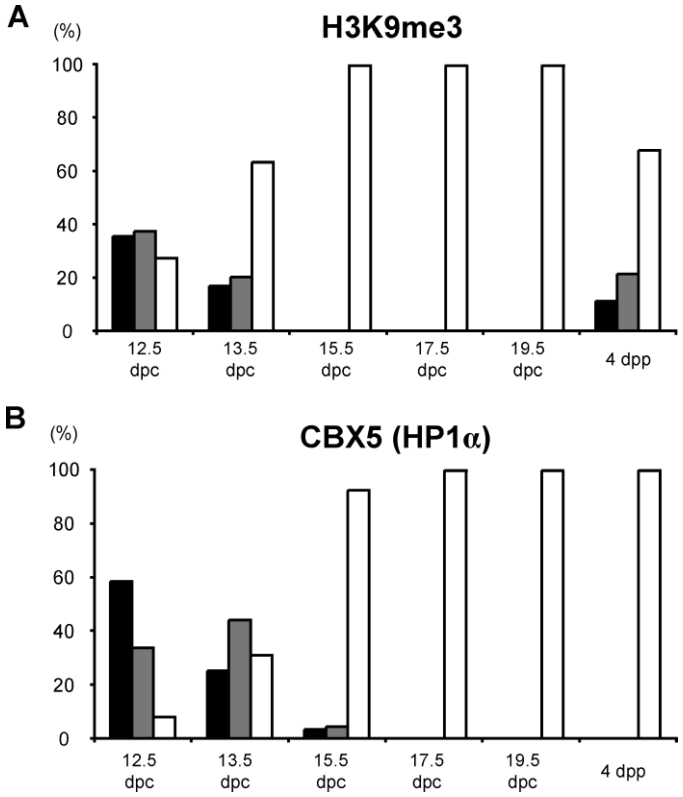


FIG. 2. The proportion of different epigenetic states during male germ cell development. **A**) The percentage of cells showing positive H3K9me3 staining in a punctate pattern (black bars), a punctate perinuclear distribution (gray bars), or a diffuse distribution (white bars) is shown. **B**) The percentage of cells showing positive CBX5 staining in a punctate pattern (black bars), a punctate perinuclear distribution (gray bars), or a diffuse distribution (white bars) is shown. At least two independent immunostaining experiments were performed and on $\geq$ 100 cells each were recorded to calculate the percentages.

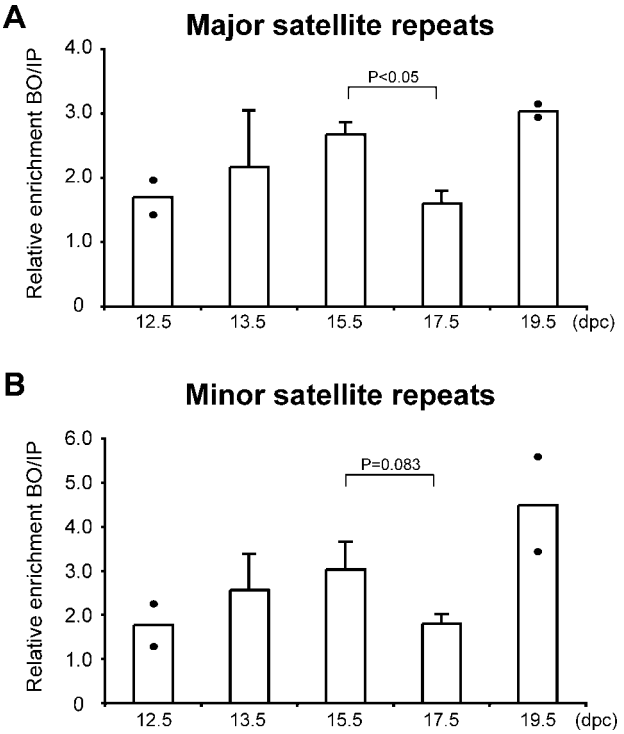


FIG. 3. Histone methylation levels at pericentric heterochromatin regions in fetal male germ cells. ChIP analyses were performed on more than 95% purified populations of fetal male germ cells recovered from specific stages prior to and during the period of mitotic arrest using an antibody specific for H3K9me3. Precipitated DNA was subjected to real-time PCR with the use of specific primers for the major satellite repeats (**A**) and minor satellite repeats (**B**), and enrichment of immunoprecipitated DNA (bound fractions [BO]) relative to input (IP) DNA was calculated in each case. Data represent mean (± SEM) values of two independent ChIP experiments for 12.5 dpc and 19.5 dpc, and more than three for 13.5 dpc, 15.5 dpc, and 17.5 dpc. Two dots show the extent of variation when only two measurements were made. Statistical analyses were performed using the Student *t*-test. A value of $P < 0.05$ was considered statistically significant.

inactive, differentiated, adult cumulus cells; and mitotically active, undifferentiated, pluripotent ES cells), and this pattern was distinct from that seen in type $T_1$ prospermatogonia. These results indicate that the pattern of nuclear organization of heterochromatin that we observed in type $T_1$ fetal prospermatogonia is indeed unique, and is common to neither all cells suspended in mitotic arrest, nor to all cells bearing a pluripotent genome.

### *The Profile of Pericentric Heterochromatin States in Developing Male Germ Cells*

The loss of chromocenter organization in type $T_1$ prospermatogonia (Fig. 1, A and B, 15.5–19.5 dpc panels) may be caused by histone hypomethylation at pericentric heterochromatin regions composed of major and minor satellite repeats. To detect epigenetic changes in constitutive heterochromatin in a region-specific manner, we assessed histone methylation levels specifically at major or minor satellite repeats by ChIP analysis (Fig. 3). Our results showed a similar, enriched abundance of H3K9me3 associated with both major and minor satellite repeats in type $T_1$ prospermatogonia. This enrichment in H3K9me3 was observed at 12.5 dpc, and continued to increase gradually until 15.5 dpc. Interestingly, this enrichment of H3K9me3 showed a transient but significant decrease across major satellite repeats at 17.5 dpc (Fig. 3A). There was a similar trend toward loss of H3K9me3 across minor satellite repeats at this same stage, although the decrease was not statistically significant (Fig. 3B). By 19.5 dpc, the level of H3K9me3 tended to be restored to previous levels. These results reveal that constitutive heterochromatin undergoes significant changes in epigenetic modifications in mitotically arrested type $T_1$ prospermatogonia.

We next examined the expression profiles in prospermatogonia of master epigenetic regulators involved in the establishment of constitutive heterochromatin, including histone methyltransferases and demethylases. The histone methyltransferases, SUV39H1 and SUV39H2, are preferentially targeted to pericentric heterochromatin to establish H3K9me3 at these regions [40, 42, 43]. On the other hand, JMJD2B is a histone demethylase that antagonizes H3K9me3 in these same regions [44, 45]. As noted above, our stage-specific ChIP assays revealed a transient loss of H3K9me3 across major and minor satellite repeats in male germ cells at 17.5 dpc (Fig. 3). To determine if this was related to changes in levels of histone methylases or demethylases, we characterized the pattern of expression of the histone-methyltransferase-encoding *Suv39h1* and *Suv39h2* genes, and of the histone-demethylase-encoding gene, *Jmjd2b*, in prospermatogonia using real-time RT-PCR (Fig. 4). Expression of *Suv39h1* was constant between 12.5 and 13.5 dpc, and then showed a transient but significant down-regulation at 15.5 dpc, followed by a gradual increase during

subsequent stages (Fig. 4A). Similarly, *Suv39h2* was also significantly down-regulated at 15.5 dpc, and then up-regulated at 17.5 dpc, but this was followed by a gradual decrease in later stages (Fig. 4B). In contrast, expression of the *Jmjd2b* gene was constant in prospermatogonia throughout fetal development, except for a transient and significant up-regulation at 17.5 dpc (Fig. 4C). Thus, the marked decrease that we observed in levels of H3K9me3 at both major and minor satellite repeats in type $T_1$ prospermatogonia at 17.5 dpc (Fig. 3) appears to correlate with a preceding decrease in levels of mRNAs encoding histone methyltransferases at 15.5 dpc (Fig. 4, A and B), and with an increase in levels of histone demethylase mRNAs at 17.5 dpc (Fig. 4C).

### *Nuclear Reorganization of Constitutive Heterochromatin in Male Germ Cells*

Our observations described above reveal a distinction between type $T_1$ prospermatogonia and adult cumulus cells. Both cell types are suspended in mitotic arrest at the $G_0/G_1$ stage, but cumulus cells retain relatively well-organized chromocenters, whereas these are lost in type $T_1$ prospermatogonia. We therefore wondered which epigenetic modifications may contribute to the loss of chromocenters in type $T_1$ prospermatogonia. We considered the possibilities that: 1) there could be a localized demethylation of H3K9me3 residues in chromatin associated uniquely with pericentric regions, resulting in a release of CBX5 protein and subsequent dissociation of the chromocenters; or 2) that this change could be associated with more global epigenomic changes in chromatin modifications in type $T_1$ prospermatogonia. We reasoned that, if the loss of organized chromocenters in type $T_1$ prospermatogonia is due to localized demethylation of H3K9me3 (option 1 above), then the pericentric regions of chromosomes should remain adjacent to one another, whereas, if the loss of organized chromocenters in these cells is due to more global epigenomic changes (option 2 above), then the pericentric regions should become more diffuse within the nuclei.

To address this question, we characterized the spatial distribution of pericentric and centromeric chromosomal regions in fetal and neonatal male germ cells using interphase FISH (Fig. 5A). In type M prospermatogonia at 12.5 dpc, pericentric and centromeric regions were detectable as small, discrete foci that were coincident with intense DAPI staining (Fig. 5A, 12.5 dpc panels). Some of these discrete foci of centromeric regions became relocated to the nuclear periphery in type $T_1$ prospermatogonia at 13.5 dpc (Fig. 5A, 13.5 dpc panels), and this pattern was then retained throughout the period of mitotic arrest in these cells (Fig. 5A, 15.5–19.5 dpc panels). In particular, type $T_1$ prospermatogonia at 17.5 dpc showed a loss of chromocenters, and diffuse distribution of pericentric and centromeric regions when analyzed by interphase FISH (Fig. 5A, 17.5 dpc panels). This was consistent with the results of our ChIP assay, which showed a transient loss of H3K9me3 at major and minor satellite repeats in these same cells (Fig. 3). However, in type $T_2$ prospermatogonia at 4 dpp (Fig. 5A, 4 dpp panels), chromocenters had become reassembled, and were clearly visible within the nucleus, similar to those observed in type M prospermatogonia at 12.5 dpc (Fig. 5A, 12.5 dpc panels).

Taken together, these results suggest that organization of pericentric heterochromatin and correlated epigenetic modifications undergo dynamic global reorganization coincident with the period of mitotic arrest in type $T_1$ prospermatogonia. This supports the second option posed above—that the disappearance of organized chromocenters in type $T_1$ prospermatogonia

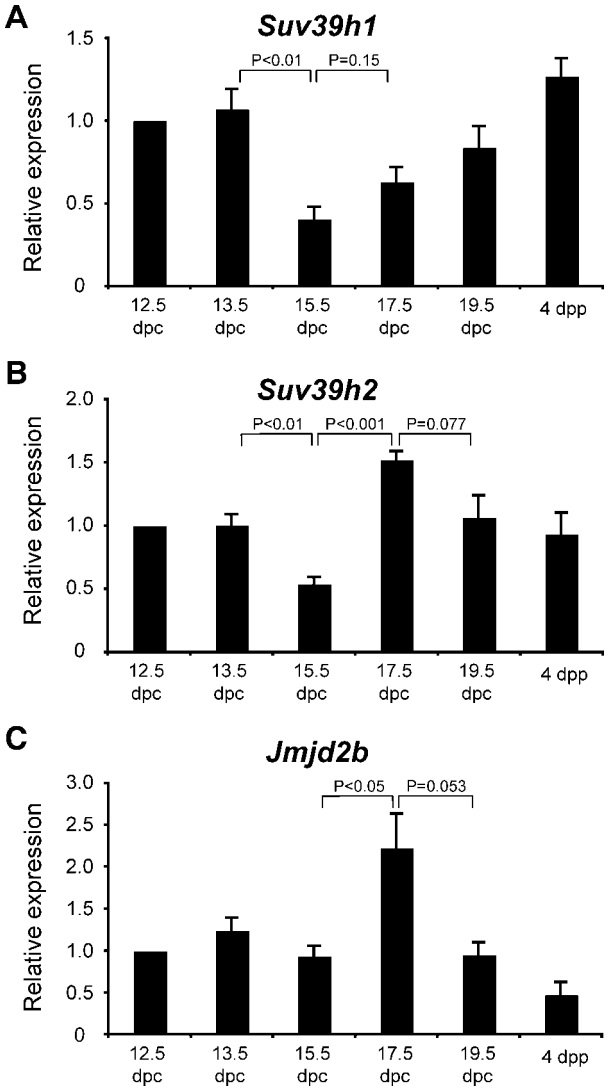


FIG. 4. Quantitative expression of two histone methyltransferase genes and a histone demethylase gene during fetal and neonatal male germ cell development. Relative expression of two different histone methyltransferase genes, *Suv39h1* (**A**) and *Suv39h2* (**B**), and a histone demethylase, *Jmjd2b* (**C**), in fetal and neonatal male germ cells are shown. In each case, expression of each gene was measured in endogenous male germ cells (recovered at 12.5, 13.5, 15.5, 17.5, and 19.5 dpc, and 4 dpp, and purified to 100%). The relative expression of each target mRNA was calculated from the target $C_T$ values and *Actb* mRNA $C_T$ values, using the standard curve method. The relative amount of each target mRNA at 12.5 dpc was arbitrarily set at 1, and all other transcript levels were compared to these values. Error bars indicate SEM. Statistical analyses were performed using the Student *t*-test. A value of $P < 0.05$ was considered statistically significant.

is associated with global changes in nuclear architecture. Interestingly, our control experiments involving cumulus cells and ES cells as examples of cells in states of mitotic arrest or pluripotency, respectively, failed to reveal a pattern of perinuclear relocation of centromeric heterochromatin (Fig. 5, B and C), indicating that the dynamic spatial reorganization of constitutive heterochromatin that we observed in prospermatogonia is a phenomenon unique to germ cells. It is intriguing to consider that this unique epigenomic phenomenon may be related to the uniquely high success previously observed in the ability of nuclei from type $T_1$ prospermatogonia to direct preimplantation development following nuclear transfer [21, 22].

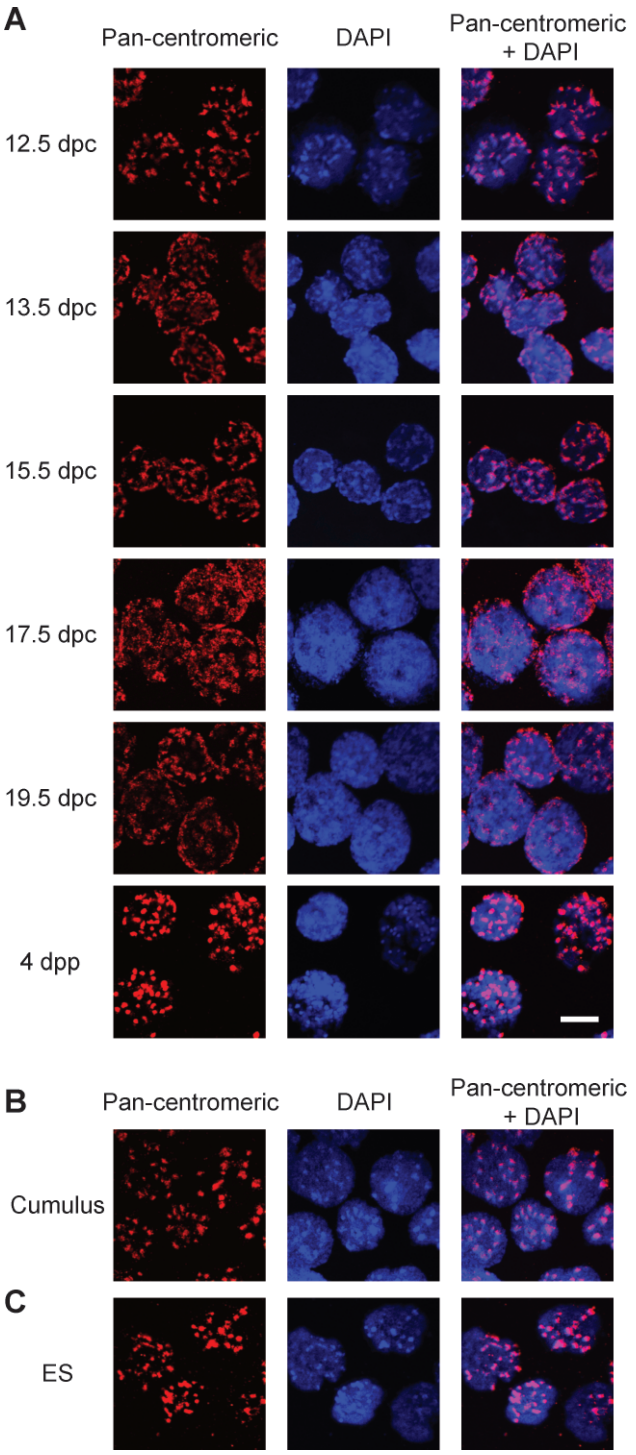


FIG. 5. Changes in nuclear architecture during prespermatogenesis. **A**) Dynamic reorganization of pericentric heterochromatin domains during fetal and neonatal male germ cell development. Male germ cells were isolated from fetuses at 12.5, 13.5, 15.5, 17.5, and 19.5 dpc, and neonates at 4 dpp, and hybridized with a Cy3-labeled pancentromeric probe (red) to visualize the nuclear localization of centromeric regions. DNA was stained with DAPI (blue). **B** and **C**) Localization of centromeric regions in cumulus cells (**B**) and in ES cells (**C**). Bar = 10 μm.

## DISCUSSION

We have examined the status of intranuclear heterochromatin organization and epigenetic markers in fetal and neonatal prospermatogonia, including mitotically active type M prospermatogonia at 12.5–13.5 dpc, mitotically arrested type $T_1$ prospermatogonia at 15.5–19.5 dpc, and type $T_2$ prospermatogonia at 4 dpp following reactivation of mitotic activity. We observed dynamic changes in heterochromatin organization and epigenetic markers associated with constitutive heterochromatin in these cells that coincided with transitions between states of mitotic activity and inactivity, and with a major period of epigenetic reprogramming. As noted above, these changes in organization of heterochromatin also coincided with changes in the capacity of nuclei from each of these cell types to sustain preimplantation and early postimplantation development of cloned embryos.

Recently, Western et al. [7] examined the precise timing and dynamics of cell cycle arrest in fetal male germ cells. Using FACS analysis based on propidium iodide staining, they found that 38%, 55%, and 95% of germ cells were arrested in the $G_0/G_1$ stage at 12.5 dpc, 13.5 dpc, and 14.5 dpc, respectively. These proportions of male germ cells found in mitotic arrest at each fetal stage were similar to those that we observed of germ cells showing diffuse staining of H3K9me3, CBX5, and DAPI (pattern no. 3, Fig. 1, A and B, 15.5–19.5 dpc panels) at these same stages, suggesting a direct link between entry into mitotic arrest and the appearance of diffuse intranuclear localization of H3K9me3- and CBX5-positive heterochromatin, along with the disappearance of the chromocenter in type $T_1$ prospermatogonia. Interestingly, a similar observation has been reported in mitotically quiescent B lymphocytes, which, like quiescent germ cells, lack certain features of nuclear heterochromatin organization, and show higher reprogramming potential compared with the same cell type following stimulation of mitotic activity [34]. However, this epigenetic feature does not appear to be common to all cells arrested in the $G_0/G_1$ phase of the cell cycle, as demonstrated by our analysis of cumulus cells that are arrested in $G_0/G_1$, but showed punctate distribution of H3K9me3 and CBX5, along with the presence of a chromocenter (Fig. 1C).

Taken together, these observations suggest that multiple parameters influence the likelihood of successful development of cloned embryos produced by nuclear transfer. One parameter is mitotic activity. Clearly, cloned embryos produced from donor cells suspended in mitotic arrest typically show higher developmental success than those produced from mitotically active cells [46]. A second parameter is genomic imprinting. Previous studies have demonstrated that embryos produced from donor germ cells in which imprints have been erased are able to develop to early-stage fetuses, but undergo severe growth retardation thereafter [20–22]. Our studies reported here, along with our previous cloning experiments using prospermatogonia as nuclear donors, suggest that a third parameter that influences developmental success of cloned embryos is the status of epigenetic programming of the genome, as indicated by nuclear organization of heterochromatin. Thus, while cumulus cells have been successfully used as somatic cell nuclear transfer donors to produce viable cloned offspring [47, 48], it is interesting to note that the percentage of cloned embryos generated from cumulus donor nuclei that developed to the morula/blastocyst stage was only 31% and 60% in two independent experiments using B6D2F1 donor cells [48]. In contrast, although no viable cloned offspring were produced when prospermatogonia were used as nuclear donors, due to a lack of proper imprinting, 100% of cloned embryos produced with nuclei from B6D2F1 type $T_1$ prospermatogonia developed to the morula/blastocyst stage [22]. This suggests that type $T_1$ prospermatogonia exist in an epigenetic state that is better predisposed to direct preimplantation development than are cumulus cells. We suggest that the differences that we

observed in intranuclear organization of heterochromatin in these two cell types are indicative of this epigenetic distinction.

Specifically, we observed that pericentric regions lost their association with H3K9me3 and CBX5 proteins, and relocated toward the nuclear periphery, and that the chromocenter became less organized in type $T_1$ prospermatogonia. Our studies of the expression profiles of histone methyltransferases (*Suv39h1* and *Suv39h2*) and histone demethylase (*Jmjd2b*) in prospermatogonia suggest that the changes that we observed in heterochromatin organization in these cells are developmentally regulated events. SUV39H histone methyltransferases govern accumulation of H3K9me3 at pericentric heterochromatin, and recruit binding of CBX5 proteins to form stable heterochromatin, and CBX5 proteins self-associate and interact with SUV39H to form a positive feedback loop [49]. SUV39H histone methyltransferases also direct Dnmt3b-dependent DNA methylation at pericentric repeats [40]. Furthermore, recent discoveries have uncovered a role for the RNA interference pathway in heterochromatin formation [30]. Given these facts, it is evident that the reorganization of pericentric heterochromatin depends on a complex and interactive modulation of epigenetic factors.

We also observed a decrease in expression of the *Suv39h* genes in type $T_1$ prospermatogonia at 15.5 dpc (Fig. 4, A and B), prior to the transient loss of H3K9me3 at 17.5 dpc (Fig. 3). While these events appear to represent a cause-and-effect relationship, it is not clear why there is a lag between the putative cause and its effect. However, it seems likely that an active DNA demethylase and/or histone demethylase is required to remodel the pericentric heterochromatin without DNA replication in male germ cells at these stages. Indeed, we observed transient activation of *Jmjd2b* gene expression in these same cells at 17.5 dpc (Fig. 4C). Interestingly, the level of H3K9me3 in germ cells at 17.5 dpc was similar to that in germ cells at 12.5 dpc (Fig. 3), even though the H3K9me3 staining patterns were different (Fig. 1). This indicates that the level of H3K9me3 is not the sole determinant of formation of the chromocenter. It will be necessary to perform knockout or knockdown studies of these key epigenetic modifiers in vivo to fully dissect the dynamic mechanism(s) governing the organization of pericentric heterochromatin and chromocenter formation during male germ cell development. However, we suspect that the changes that we observed in expression of genes encoding key epigenetic modifiers may initiate a series of changes in components of constitutive heterochromatin or their modified states that result in diffusion of heterochromatin throughout the nucleus.

The notion that heterochromatin organization is indicative of reprogramming potential is supported by previous observations including a report by Houlard et al. [50] that showed that ES cells depleted of chromatin assembly factor 1 underwent a loss of chromocenter organization and delocalization of CBX5, with a relocation of centromeric and pericentric heterochromatin to the nuclear periphery. Another report by Taddei et al. [51] showed that long-term treatment of mouse fibroblast L929 cells or human HeLa cells with the histone deacetylase inhibitor, trichostatin A, reversibly induced the relocation of centromeric regions at the nuclear periphery, with loss of chromocenter organization and delocalization of CBX5. The results of our analysis of the spatial distribution of pericentric and centromeric chromosomal regions in fetal and neonatal male germ cells suggest that these effects may be correlated with more general epigenetic changes in chromatin structure that render the genome in a donor nucleus more amenable to reprogramming cues emanating from the ooplasm of the recipient enucleated oocyte following nuclear transfer.

Previous studies have documented at least two periods of genome-wide epigenetic reprogramming during fetal germ cell development in the mouse. The first occurs at about 8.5 dpc, when PGCs are migrating, and may be necessary for eventual transmission of genomic totipotency to the zygote [12–14]. The second reprogramming event occurs at about 11.5 dpc, coincident with the arrival of PGCs in the developing gonads, and includes genome-wide DNA demethylation, and major changes in nuclear architecture accompanied by an extensive erasure of several histone modifications [18]. This step appears to be crucial for erasure of genomic imprints. Genome-wide chromatin reprogramming then continues during postnatal spermatogenesis, including meiosis and spermatid differentiation [19]. The functional significance of H3K9me3 at pericentric regions during meiosis is evident in mice with deletions of both *Suv39h1* and *Suv39h2* genes [43]. In these double-mutant mice, genomic stability is impaired, with differentiation arrest at the transition between early-to-late spermatocytes, resulting in severe impairment of spermatogenesis. Recently, Govin et al. [52] showed a distinct behavior of pericentric heterochromatin during postmeiotic chromatin reorganization in male germ cells. Pericentric regions are dynamically reorganized in elongating spermatids to acquire a unique epigenetic state, marked by both histone H4 acetylation and H3K9me3, and loss of CBX5. These unique epigenetic marks may be required to establish sperm-specific packaging of pericentric heterochromatin in condensed nuclei.

In the present study, we reveal yet another period of epigenetic reprogramming in male germ cells during the late fetal/early postnatal stages. This reprogramming is characterized by global changes in chromatin conformation in type $T_1$ prospermatogonia that correlate with the timing of re-establishment of biallelic imprints in the male germ line that are a critical prerequisite for developmental competence in the paternal genome [15, 19]. Thus, we suggest that a global decondensation of chromatin conformation occurs in type $T_1$ prospermatogonia, and is normally required to facilitate paternal imprinting, but also represents an epigenetic state that is particularly amenable to efficient reprogramming upon nuclear transfer. While the initial observations that we have reported here clearly warrant significant follow-up studies, we believe that we have described evidence of a unique epigenetic state in prospermatogonia. In addition, this information may be useful in efforts to understand the normal process of epigenetic reprogramming that occurs during male gametogenesis, as well as the molecular basis of epigenetic reprogramming of differentiated cells required to achieve a pluripotent state.

## ACKNOWLEDGMENTS

We are grateful to Drs. Jeffrey R. Mann (University of Melbourne, Melbourne, Australia) for providing *Pou5f1*-GFP-transgenic mice, Richard Allsopp (University of Hawaii) for providing embryonic stem cells, and Satoshi Namekawa (Massachusetts General Hospital, Harvard Medical School) for technical advice on immunocytochemistry. We also thank Ms. Alexandra Gurary (University of Hawaii) for assistance with FACS sorting.

## REFERENCES

1. Ohinata Y, Payer B, O'Carroll D, Ancelin K, Ono Y, Sano M, Barton SC, Obukhanych T, Nussenzweig M, Tarakhovsky A, Saitou M, Surani MA. Blimp1 is a critical determinant of the germ cell lineage in mice. Nature 2005; 436:207–213.
2. McCarrey JR. Development of the germ cell. In: Desjardins C, Ewing LL (eds.), Cell and Molecular Biology of the Testis. New York: Oxford University Press; 1993:58–89.
3. McLaren A. Primordial germ cells in the mouse. Dev Biol 2003; 262:1–15.
4. Koopman P, Münsterberg A, Capel B, Vivian N, Lovell-Badge R.

Expression of a candidate sex-determining gene during mouse testis differentiation. Nature 1990; 348:450–452.
5. Wilhelm D, Koopman P. The makings of maleness: towards an integrated view of male sexual development. Nat Rev Genet 2006; 7:620–631.
6. Svingen T, Koopman P. Involvement of homeobox genes in mammalian sexual development. Sex Dev 2007; 1:12–23.
7. Western PS, Miles DC, van den Bergen JA, Burton M, Sinclair AH. Dynamic regulation of mitotic arrest in fetal male germ cells. Stem Cells 2008; 26:339–347.
8. Kafri T, Ariel M, Brandeis M, Shemer R, Urven L, McCarrey J, Cedar H, Razin A. Developmental pattern of gene-specific DNA methylation in the mouse embryo and germ line. Genes Dev 1992; 6:705–714.
9. Davis TL, Yang GJ, McCarrey JR, Bartolomei MS. The H19 methylation imprint is erased and re-established differentially on the parental alleles during male germ cell development. Hum Mol Genet 2000; 9:2885–2894.
10. Ueda T, Abe K, Miura A, Yuzuriha M, Zubair M, Noguchi M, Niwa K, Kawase Y, Kono T, Matsuda Y, Fujimoto H, Shibata H, et al. The paternal methylation imprint of the mouse H19 locus is acquired in the gonocyte stage during foetal testis development. Genes Cells 2000; 5:649–659.
11. Szabó PE, Hübner K, Schöler H, Mann JR. Allele-specific expression of imprinted genes in mouse migratory primordial germ cells. Mech Dev 2002; 115:157–160.
12. Seki Y, Hayashi K, Itoh K, Mizugaki M, Saitou M, Matsui Y. Extensive and orderly reprogramming of genome-wide chromatin modifications associated with specification and early development of germ cells in mice. Dev Biol 2005; 278:440–458.
13. Seki Y, Yamaji M, Yabuta Y, Sano M, Shigeta M, Matsui Y, Saga Y, Tachibana M, Shinkai Y, Saitou M. Cellular dynamics associated with the genome-wide epigenetic reprogramming in migrating primordial germ cells in mice. Development 2007; 134:2627–2638.
14. Ancelin K, Lange UC, Hajkova P, Schneider R, Bannister AJ, Kouzarides T, Surani MA. Blimp1 associates with Prmt5 and directs histone arginine methylation in mouse germ cells. Nat Cell Biol 2006; 8:623–630.
15. Jelinic P, Stehle JC, Shaw P. The testis-specific factor CTCFL cooperates with the protein methyltransferase PRMT7 in H19 imprinting control region methylation. PLoS Biol 2006; 4:e355.
16. Trasler JM. Gamete imprinting: setting epigenetic patterns for the next generation. Reprod Fertil Dev 2006; 18:63–69.
17. Kato Y, Kaneda M, Hata K, Kumaki K, Hisano M, Kohara Y, Okano M, Li E, Nozaki M, Sasaki H. Role of the Dnmt3 family in de novo methylation of imprinted and repetitive sequences during male germ cell development in the mouse. Hum Mol Genet 2007; 16:2272–2280.
18. Hajkova P, Ancelin K, Waldmann T, Lacoste N, Lange UC, Cesari F, Lee C, Almouzni G, Schneider R, Surani MA. Chromatin dynamics during epigenetic reprogramming in the mouse germ line. Nature 2008; 452:877–881.
19. Sasaki H, Matsui Y. Epigenetic events in mammalian germ-cell development: reprogramming and beyond. Nat Rev Genet 2008; 9:129–140.
20. Kato Y, Rideout WM III, Hilton K, Barton SC, Tsunoda Y, Surani MA. Developmental potential of mouse primordial germ cells. Development 1999; 126:1823–1832.
21. Lee J, Inoue K, Ono R, Ogonuki N, Kohda T, Kaneko-Ishino T, Ogura A, Ishino F. Erasing genomic imprinting memory in mouse clone embryos produced from day 11.5 primordial germ cells. Development 2002; 129: 1807–1817.
22. Yamazaki Y, Mann MR, Lee SS, Marh J, McCarrey JR, Yanagimachi R, Bartolomei MS. Reprogramming of primordial germ cells begins before migration into the genital ridge, making these cells inadequate donors for reproductive cloning. Proc Natl Acad Sci U S A 2003; 100:12207–12212.
23. Miki H, Inoue K, Kohda T, Honda A, Ogonuki N, Yuzuriha M, Mise N, Matsui Y, Baba T, Abe K, Ishino F, Ogura A. Birth of mice produced by germ cell nuclear transfer. Genesis 2005; 41:81–86.
24. Yamazaki Y, Low EW, Marikawa Y, Iwahashi K, Bartolomei MS, McCarrey JR, Yanagimachi R. Adult mice cloned from migrating primordial germ cells. Proc Natl Acad Sci U S A 2005; 102:11361–11366.
25. Li E. Chromatin modification and epigenetic reprogramming in mammalian development. Nat Rev Genet 2002; 3:662–673.
26. Ekwall K. Epigenetic control of centromere behavior. Annu Rev Genet 2007; 41:63–81.
27. Maison C, Bailly D, Peters AH, Quivy JP, Roche D, Taddei A, Lachner M, Jenuwein T, Almouzni G. Higher-order structure in pericentric heterochromatin involves a distinct pattern of histone modification and an RNA component. Nat Genet 2002; 30:329–334.
28. Nielsen AL, Oulad-Abdelghani M, Ortiz JA, Remboutsika E, Chambon P, Losson R. Heterochromatin formation in mammalian cells: interaction between histones and HP1 proteins. Mol Cell 2001; 7:729–739.
29. Maison C, Almouzni G. HP1 and the dynamics of heterochromatin maintenance. Nat Rev Mol Cell Biol 2004; 5:296–304.
30. Grewal SI, Jia S. Heterochromatin revisited. Nat Rev Genet 2007; 8:35–46.
31. Guenatri M, Bailly D, Maison C, Almouzni G. Mouse centric and pericentric satellite repeats form distinct functional heterochromatin. J Cell Biol 2004; 166:493–505.
32. Meshorer E, Yellajoshula D, George E, Scambler PJ, Brown DT, Misteli T. Hyperdynamic plasticity of chromatin proteins in pluripotent embryonic stem cells. Dev Cell 2006; 10:105–116.
33. Kobayakawa S, Miike K, Nakao M, Abe K. Dynamic changes in the epigenomic state and nuclear organization of differentiating mouse embryonic stem cells. Genes Cells 2007; 12:447–460.
34. Baxter J, Sauer S, Peters A, John R, Williams R, Caparros ML, Arney K, Otte A, Jenuwein T, Merkenschlager M, Fisher AG. Histone hypomethylation is an indicator of epigenetic plasticity in quiescent lymphocytes. EMBO J 2004; 23:4462–4472.
35. Brero A, Easwaran HP, Nowak D, Grunewald I, Cremer T, Leonhardt H, Cardoso MC. Methyl CpG-binding proteins induce large-scale chromatin reorganization during terminal differentiation. J Cell Biol 2005; 169:733–743.
36. Terranova R, Sauer S, Merkenschlager M, Fisher AG. The reorganisation of constitutive heterochromatin in differentiating muscle requires HDAC activity. Exp Cell Res 2005; 310:344–356.
37. Nagy A. Manipulating the Mouse Embryo: A Laboratory Manual. Cold Spring Harbor, NY: Cold Spring Harbor Laboratory Press; 2003.
38. Stewart CL. Production of chimeras between embryonic stem cells and embryos. Methods Enzymol 1993; 225:823–855.
39. O'Neill LP, VerMilyea MD, Turner BM. Epigenetic characterization of the early embryo with a chromatin immunoprecipitation protocol applicable to small cell populations. Nat Genet 2006; 38:835–841.
40. Lehnertz B, Ueda Y, Derijck AA, Braunschweig U, Perez-Burgos L, Kubicek S, Chen T, Li E, Jenuwein T, Peters AH. Suv39h-mediated histone H3 lysine 9 methylation directs DNA methylation to major satellite repeats at pericentric heterochromatin. Curr Biol 2003; 13:1192–1200.
41. Schuetz AW, Whittingham DG, Snowden R. Alterations in the cell cycle of mouse cumulus granulosa cells during expansion and mucification in vivo and in vitro. Reprod Fertil Dev 1996; 8:935–943.
42. O'Carroll D, Scherthan H, Peters AH, Opravil S, Haynes AR, Laible G, Rea S, Schmid M, Lebersorger A, Jerratsch M, Sattler L, Mattei MG, et al. Isolation and characterization of Suv39h2, a second histone H3 methyltransferase gene that displays testis-specific expression. Mol Cell Biol 2000; 20:9423–9433.
43. Peters AH, O'Carroll D, Scherthan H, Mechtler K, Sauer S, Schöfer C, Weipoltshammer K, Pagani M, Lachner M, Kohlmaier A, Opravil S, Doyle M, et al. Loss of the Suv39h histone methyltransferases impairs mammalian heterochromatin and genome stability. Cell 2001; 107:323–337.
44. Fodor BD, Kubicek S, Yonezawa M, O'Sullivan RJ, Sengupta R, Perez-Burgos L, Opravil S, Mechtler K, Schotta G, Jenuwein T. Jmjd2b antagonizes H3K9 trimethylation at pericentric heterochromatin in mammalian cells. Genes Dev 2006; 20:1557–1562.
45. Klose RJ, Kallin EM, Zhang Y. JmjC-domain-containing proteins and histone demethylation. Nat Rev Genet 2006; 7:715–727.
46. Campbell KH. Nuclear transfer in farm animal species. Semin Cell Dev Biol 1999; 10:245–252.
47. Wakayama T, Perry AC, Zuccotti M, Johnson KR, Yanagimachi R. Full-term development of mice from enucleated oocytes injected with cumulus cell nuclei. Nature 1998; 394:369–374.
48. Wakayama T, Yanagimachi R. Mouse cloning with nucleus donor cells of different age and type. Mol Reprod Dev 2001; 58:376–383.
49. Aagaard L, Laible G, Selenko P, Schmid M, Dorn R, Schotta G, Kuhfittig S, Wolf A, Lebersorger A, Singh PB, Reuter G, Jenuwein T. Functional mammalian homologues of the Drosophila PEV-modifier Su(var)3–9 encode centromere-associated proteins which complex with the heterochromatin component M31. EMBO J 1999; 18:1923–1938.
50. Houlard M, Berlivet S, Probst AV, Quivy JP, Héry P, Almouzni G, Gérard M. CAF-1 is essential for heterochromatin organization in pluripotent embryonic cells. PLoS Genet 2006; 2:e181.
51. Taddei A, Maison C, Roche D, Almouzni G. Reversible disruption of pericentric heterochromatin and centromere function by inhibiting deacetylases. Nat Cell Biol 2001; 3:114–120.
52. Govin J, Escoffier E, Rousseaux S, Kuhn L, Ferro M, Thevenon J, Catena R, Davidson I, Garin J, Khochbin S, Caron C. Pericentric heterochromatin reprogramming by new histone variants during mouse spermiogenesis. J Cell Biol 2007; 176:283–294.